A density functional theory study of hydroxyl and the intermediate in the water formation reaction on Pt

A. Michaelides and P. Hu

Citation: The Journal of Chemical Physics **114**, 513 (2001); doi: 10.1063/1.1328746
View online: http://dx.doi.org/10.1063/1.1328746
View Table of Contents: http://scitation.aip.org/content/aip/journal/jcp/114/1?ver=pdfcov
Published by the AIP Publishing

A density functional theory study of hydroxyl and the intermediate in the water formation reaction on Pt

A. Michaelides and P. Hu[a)]
School of Chemistry, The Queen's University of Belfast, Belfast BT9 5AG, United Kingdom

(Received 21 August 2000; accepted 5 October 2000)

Density functional theory has been used to study the adsorption of hydroxyl at low and high coverages and also to investigate the nature of the intermediate in the H_2O formation reaction on Pt(111). At low coverages [1/9 of a monolayer (ML) to 1/3 ML] OH binds preferentially at bridge and top sites with a chemisorption energy of ~2.25 eV. At high coverages (1/2 ML to 1 ML) H bonding between adjacent hydroxyls causes: (i) an enhancement in OH chemisorption energy by about 15%; (ii) a strong preference for OH adsorption at top sites; and (iii) the formation of OH networks. The activation energy for the diffusion of isolated OH groups along close packed rows of Pt atoms is 0.1 eV. This low barrier coupled with H bonding between neighboring OH groups indicates that hydroxyls are susceptible to island formation at low coverages. Pure OH as well as coadsorbed OH and H can be ruled out as the observed low temperature intermediate in the water formation reaction. Instead we suggest that the intermediate consists of a mixed $OH+H_2O$ overlayer with a macroscopic surface coverage of 3/4 ML in a 2:1 ratio of OH and H_2O. © *2001 American Institute of Physics.* [DOI: 10.1063/1.1328746]

I. INTRODUCTION

Adsorbed hydroxyl groups play a crucial role in an enormous number of chemical processes. They are important to electrochemistry and heterogeneous catalysis and are intermediates in all catalytic combustion processes involving H containing fuels over transition metal surfaces. Consequently, OH groups have been intensively investigated. Given their transitory nature, however, reports concerning their interaction with metal surfaces are conflicting.

Fisher and Sexton[1] were the first to report the observation of chemisorbed OH. They suggested that OH, on Pt(111), could be prepared by adsorption of H_2O on an O covered surface at 100 K followed by annealing to 150 K. Vibrational and electronic spectra showed features which could be interpreted as being due to adsorbed OH. It was, therefore, suggested that H_2O and O disproportionate to produce OH. This method is now routinely used to produce OH covered surfaces.[2–9] In subsequent studies, Creighton and White[2] concluded from isotopically labeled thermal desorption experiments that the stoichiometry of the disproportionation reaction between H_2O and O was 2:1 and suggested that the OH producing reaction on Pt(111) was:

$$2H_2O_{(ads)}+O_{(ads)}\rightarrow 3OH_{(ads)}+H_{(ads)}. \quad (1)$$

An area in which OH groups play a critical role is the hydrogen-oxidation to water reaction. This process dates back to the time of Faraday[10,11] and constitutes a fundamental reaction step in many catalytic processes of industrial importance. The mechanism of this reaction and the nature of the intermediate through which it proceeds have been intensively debated over the years.[12–23] Recently, Ertl and coworkers have studied the water formation reaction on Pt(111).[3] With the scanning tunneling microscope (STM) this process was seen to proceed, at <180 K, through reaction fronts. The following reaction mechanism was proposed:

$$O_{(ads)}+H_{(ads)}\rightarrow OH_{(ads)}, \quad (2)$$

$$OH_{(ads)}+H_{(ads)}\rightarrow H_2O_{(ads)}, \quad (3)$$

$$H_2O_{(ads)}+O_{(ads)}\rightarrow 2OH_{(ads)}. \quad (4)$$

Step 2 initiates the process and the bulk of the H_2O is formed by cyclic repetition of hydrogenation [reaction (3)] and disproportionation [reaction (4)] steps. In a subsequent study[4] they showed that the stoichiometry of the disproportionation step was again $2H_2O$ to 1O. Furthermore, they demonstrated conclusively that the intermediate which propagates across the surface in the reaction fronts is the *same* species that is produced after coadsorption of $2H_2O$ and 1O [reaction (1)]. Using STM and low energy electron diffraction (LEED) they also showed that this species, with an overall surface coverage of 3/4 of a monolayer (ML), contained majority regions with $\sqrt{3}\times\sqrt{3}$-*R*30° and/or (3×3) periodicity and minority (1×1) domains. A structural model was proposed with this species characterized as chemisorbed OH. One can imply from reaction (1), however, that additional H atoms should also be present upon the surface although these were never detected by either STM or HREELS and are not included in structural models. In the present study we wish to investigate the nature of these ordered phases and hope to ''find'' the missing H atoms.

Theoretical calculations have been widely employed in the study of catalytic reaction intermediates.[24–28] Previous work on OH, however, has been performed on cluster models and has focused on the adsorption of isolated hydroxyls.

a)Author to whom correspondence should be addressed. Electronic mail: p.hu@qub.ac.uk

Van Santen and co-workers[29] have performed density functional theory (DFT) cluster calculations for OH chemisorption on a variety of transition and noble metal surfaces. They found that OH binds preferentially at three-fold hollow sites and calculated chemisorption energies to lie in the 1.8–3 eV range. Hermann *et al.*[30] have performed *ab initio* Hartree–Fock linear-combination-of-atomic-orbitals calculations for OH chemisorption on Cu(111) cluster models. They found that the fcc three-fold hollow sites are energetically favored with a chemisorption energy of 3.1 eV. An analysis of the metal-OH chemisorption bond identified considerable metal to OH charge transfer. Yang and Whitten[31,32] have performed embedded cluster configuration interaction (CI) calculations for OH chemisorption on Fe(110), Ni(111), and Ni(110). Optimised structures and chemisorption energies were reported for OH adsorption at the various high symmetry sites. The high coordination sites were found to be the most stable sites for OH adsorption with chemisorption energies of about 4 eV on all surfaces. Patrito *et al.*[33] have applied the bond-order conservation Morse potential method (BOC-MP) to the energetics of OH chemisorption on Ni, Pd, Pt, and Rh. Calculated chemisorption energies at zero coverage were 2.64, 1.74, 1.67, and 2.21 eV on Ni, Pd, Pt, and Rh, respectively.

Motivated by the recent observations of the intermediate in the H_2O formation reaction, we have performed periodic DFT calculations for OH chemisorption on Pt(111) at a range of surface coverages. In addition, we have examined the coadsorption of OH and H. This leads us, in part, to the suggestion that the intermediate in the H_2O formation reaction on Pt(111) may be $OH+H_2O$ and not pure OH or OH+H as previously believed. We briefly outline some details of our total energy calculations below. Following this there is an investigation of OH chemisorption at low and high coverages. In Sec. III B we discuss the nature of the intermediate in the water formation reaction. Our conclusions are summarized in the final section.

II. CALCULATION DETAILS

First-principle total energy calculations within the DFT framework were performed.[34] Ionic cores are described by ultra-soft pseudopotentials[35] and the Kohn–Sham one-electron states are expanded in a plane wave basis set, up to 300 eV. A Fermi smearing of 0.1 eV was utilized and the corrected energy extrapolated to zero Kelvin. The generalized gradient approximation of Perdew and Wang (PW91)[36] was used throughout.

The Pt(111) surface was modeled by a periodic array of slabs. A calculated Pt lattice constant of 3.9711 Å (experimental=3.9239 Å) was used throughout. Several different unit cells—$\sqrt{3}\times\sqrt{3}$-$R30°$ $p(2\times2)$, $p(3\times2)$ and $p(3\times3)$—were used. By variation of the unit cell and the number of OH groups in each unit cell, we investigate OH chemisorption at a wide range of coverages. Tests were conducted in order to decide on the appropriate number of Pt layers to use throughout the study. Hydroxyl chemisorption was considered at 1/4 ML coverage on a fixed two, three, and four layer slab and also on a four layer slab in which the top layer of Pt atoms were allowed to relax. From Table I it is clear that the structural parameters and chemisorption energies are similar in all systems. It was decided, therefore, to use a fixed three layer Pt slab throughout since this offered the best compromise between accuracy and computational load. The vacuum region between slabs was in excess of 11 Å. A Monkhorst Pack mesh[37] with $5\times5\times1$ **k**-point sampling in the surface Brillouin zone was used for the $\sqrt{3}\times\sqrt{3}$-$R30°$ unit cell and varied accordingly for the others.

TABLE I. Testing calculations for a bridge site OH at 1/4 ML coverage on two, three, and four layer Pt slabs. $O_\perp$ and α refer to the O surface distance and the surface O–H angle, respectively. 4(relaxed) refers to OH on a four layer Pt slab in which the top layer of Pt atoms are allowed to relax.

Pt layers	E_{ads} (eV)	O–H (Å)	O–Pt (Å)	$O_\perp$ (Å)	α (°)
2	2.24	0.98	2.17	1.66	113
3	2.22	0.98	2.17	1.66	113
4	2.20	0.98	2.17	1.66	113
4(relaxed)	2.23	0.98	2.14	1.65	110

Chemisorption energies (E_{ads}) per OH were calculated, at the various OH coverages, from

$$E_{ads}=E_{OH}+E_{Pt}-E_{OH/Pt},$$

where E_{OH}, E_{Pt}, and $E_{OH/Pt}$ are the total energies of free OH, Pt(111), and Pt(111)–OH. Vibrational modes were determined via the numerical calculation of the Hessian matrix. The Hessian matrix elements are computed through displacement of each Cartesian component of a selected set of atoms by $\pm\delta$. For each such displacement a self-consistent electronic structure calculation is performed, yielding all forces on all Cartesian componenets of atoms. The Hessian matrix element $D_{i\alpha j\beta}$ is obtained by numerical differentiation of the forces:

$$D_{i\alpha,j\beta}=\frac{1}{\sqrt{m_i m_j}}\frac{\partial F_{i\alpha}}{\partial R_{j\beta}}$$

$$\approx\frac{1}{\sqrt{m_i m_j}}\frac{F_{i\alpha}(R_{j\beta}+\delta)-F_{i\alpha}(R_{j\beta}-\delta)}{2\delta},$$

where $F_{i\alpha}(R_{j\beta}+\delta)$ is the force on atom α in the i direction ($i=x,y,z$) with atom β moving a distance δ from the optimized structure in the j direction; m_i is the mass on atom i. Testing calculations for free molecules and previous studies of adsorbed species[38] reveal that with this approach we calculate normal modes which differ from experiment by ca. 4%.

III. RESULTS AND DISCUSSION

A. OH chemisorption

Hydroxyl chemisorption was examined at eight different coverages ranging from 1/9 ML to 1 ML. OH binds quite strongly at all coverages with chemisorption energies between 2.2 and 2.53 eV. This is illustrated in Fig. 1 from which it can be seen that there are essentially two distinct coverage regimes: (i) at low OH coverages (1/9→1/3 ML) the OH chemisorption energy is ca. 2.25 eV; and (ii) at me-

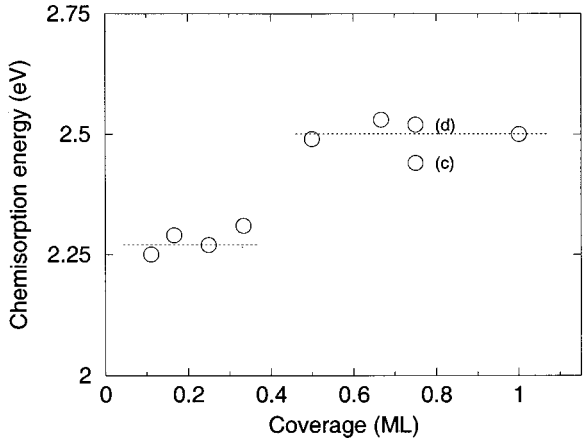

FIG. 1. Coverage dependence of OH chemisorption energy on Pt(111). At 0.75 ML two values (c and d) are given, corresponding to two different overlayers, shown in Figs. 3(c) and 3(d), considered at this coverage.

dium to high coverages (1/2→1 ML) the OH chemisorption energy is ca. 2.5 eV. Below we consider OH chemisorption in both regimes.

1. Low OH coverage (1/9→1/3 ML)

Table II lists chemisorption energies and optimized structural parameters for OH chemisorption at coverages from 1/9 to 1/3 ML. Within this coverage regime OH binds most strongly to the surface at bridge and top sites. The three-fold hollow sites are not minima in the potential energy landscape. The main properties of the adsorption systems such as those listed in Table II are alike within this coverage regime. For convenience, therefore, we restrict our discussion of OH chemisorption at low coverages to 1/4 ML.

At 1/4 ML the OH chemisorption energy is 2.27 and 2.22 eV at the top and bridge sites, respectively. Constrained structure optimizations at the fcc and hcp three-fold hollow sites, performed by fixing the O atom of OH directly above the ideal hollow site positions, revealed that these sites are ~0.3 and ~0.5 eV, respectively, less stable than the top site. Figure 2 displays the structure of OH at the top, bridge, and fcc sites. At all sites OH adsorbs with the O end down. At the bridge and top sites the OH axis makes an angle of 67° and 71°, respectively, with the surface normal. At the three-fold hollow sites the OH axis is essentially in the plane of the surface normal. The O–Pt bond length increases from 2.00 to 2.26 Å upon moving OH from the top to the hcp three-fold hollow sites. At each site the OH bond length is essentially unchanged from its gas-phase value of 0.98 Å. The most favorable orientation for OH at the top site [Fig. 2(a)] is to have the OH bond inclined toward a bridge site. The potential energy surface for rotation of OH about the surface normal at this site is fairly flat, however, with a barrier of 0.05 eV.

TABLE II. Chemisorption energies and selected structural parameters for low coverage (1/9 ML→1/3 ML) OH adsorption on Pt(111). $O_\perp$ and α refer to the O surface distance and the surface O–H angle, respectively.

Coverage (ML)	Site	E_{ads} (eV)	O–H (Å)	O–Pt (Å)	$O_\perp$ (Å)	α (°)
1/9	bridge	2.23	0.98	2.17	1.66	113
1/9	top	2.25	0.97	2.00	2.00	107
1/6	bridge	2.24	0.98	2.17	1.66	113
1/6	top	2.29	0.98	2.00	2.00	107
1/4	bridge	2.22	0.98	2.17	1.66	113
1/4	top	2.27	0.97	2.00	2.00	109
1/4	fcc	2.00	0.97	2.20	1.49	179
1/4	hcp	1.80	0.97	2.26	1.58	177
1/3	bridge	2.26	0.98	2.17	1.66	112
1/3	top	2.31	0.98	2.00	2.00	108

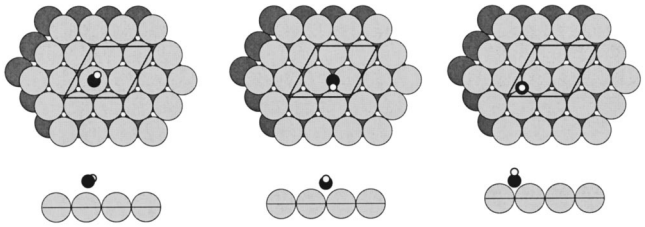

FIG. 2. Low coverage structures of OH adsorbed at the top, bridge, and fcc sites of Pt(111). Gray, black, and white circles correspond to Pt, O, and H atoms, respectively. Only two surface layers are shown for clarity. The solid lines represent the surface unit cell.

We have investigated the diffusion of OH across the Pt(111) surface at 1/4 ML. A barrier of 0.11 eV has been determined for the diffusion of OH between bridge and top sites. Hydroxyl will, therefore, be capable of diffusing easily along close packed rows of Pt atoms. Such easy diffusion coupled with an enhancement in chemisorption energy at higher OH coverages indicates that hydroxyls will tend to cluster and form islands at low surface coverages.

2. Medium-to-high OH coverage (1/2→1 ML)

Within this coverage regime hydroxyls bind to the surface with a chemisorption energy of ca. 2.5 eV (Fig. 1). This 15% enhancement in the chemisorption energy compared to low OH coverages is due to H bonding interactions between neighboring OH groups. Patrito *et al.*[33] have applied the BOC-MP method to the energetics of H bonding in adsorbed hydroxyls. For the specific case of 1/2 ML OH on Pt, the BOC-MP method predicts that H bonding will cause an increase in the OH chemisorption energy to 2.55 eV from a zero coverage value of 1.67 eV. We find, in fact, that H bonding is of crucial importance not only to the energetics but also to the structure of hydroxyl overlayers. Within this coverage regime the most stable overlayer is always the one that allows for the most effective H bonding interactions. This tends to result in the formation of OH ''chains'' and in a clear preference for OH chemisorption at top sites.

The most stable OH structure at each coverage is shown in Fig. 3 and the optimized structural parameters for these phases are listed in Table III. In general, the values for O–Pt distance and OH tilt angle for individual OH groups within these phases are similar to their respective values at low OH coverages. The O–H bond lengths tend to be slightly elongated (0.99–1.00 Å) compared to low OH coverages, which is an indication of H bonding.

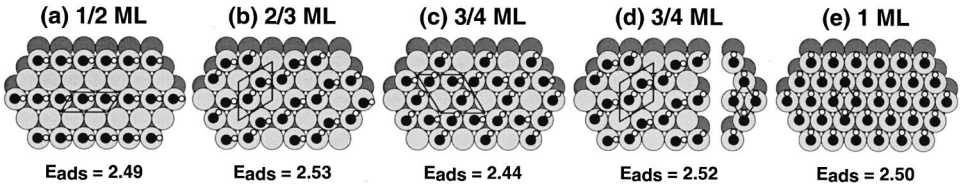

FIG. 3. Plan views of the most stable high coverage (1/2 ML→1 ML) pure OH phases on Pt(111). (d) illustrates how 3/4 ML OH can be partitioned into majority $\sqrt{3}\times\sqrt{3}-R30°$ (76%) and minority (1×1) (24%) domains.

At this juncture we shall consider each phase in turn. At 1/2 ML OH groups bind with a chemisorption energy of 2.49 eV to top sites and form linear chains with (2×1) periodicity [Fig. 3(a)]. The chains run along close packed rows of Pt atoms with each OH group pointing directly toward an antecedent OH.

Two-third ML is the OH coverage in the experimentally observed majority $\sqrt{3}\times\sqrt{3}$-$R30°$ and (3×3) domains. $\sqrt{3}\times\sqrt{3}$-$R30°$ and (3×3) domains coexist and, except for the different periodicity, which has been attributed only to local rearrangements of OH groups, there is a close similarity between both structures.[4] Because of this and the greater computational load involved in studying the (3×3) phase, we have chosen to investigate only the $\sqrt{3}\times\sqrt{3}$-$R30°$ phase. We find that the $\sqrt{3}\times\sqrt{3}$-$R30°$ phase is the most stable OH phase at any coverage with a chemisorption energy of 2.53 eV per OH. OH groups bind to top sites and form ''zigzag''-like chains across the surface [Fig. 3(b)]. This, with the added local structural information in Table III, is essentially the same as the structural model suggested by Ertl and coworkers for the $\sqrt{3}\times\sqrt{3}$-$R30°$ domains.[4] Since this is the most stable OH phase calculated for any coverage, and it agrees with the structural model proposed by Ertl and coworkers, one would be inclined to believe that this is, indeed, the nature of the observed $\sqrt{3}\times\sqrt{3}$-$R30°$ domains. Such an assignment, however, neglects the presence of additional H atoms which we can imply from Eq. 1. We will show in Sec. III B that the inclusion of the additional H atoms is essential in understanding the true chemical nature of this phase.

Three-fourth ML is the overall experimental coverage for the observed OH overlayer.[4] We have treated OH adsorption at this coverage in two distinct ways. We first considered OH adsorption with a uniform coverage of 3/4 ML. This yields the OH phase shown in Fig. 3(c), which is the least stable of the high coverage OH phases with a chemisorption energy of 2.44 eV per OH. The structure of this phase can be viewed as (2×1)OH chains with additional hydroxyls sitting on one of the two free Pt atoms of each surface $p(2\times2)$ unit cell. The second method used to model 3/4 ML OH coverage is to recreate the experimentally observed 3/4 ML overlayer more precisely. As mentioned earlier, hydroxyls are partitioned into majority $\sqrt{3}\times\sqrt{3}$-$R30°$ and/or (3×3) phases with local coverage 2/3 ML and minority (1×1) phases. If the overall surface coverage is exactly 3/4 ML then 76% and 24% of the surface will be covered in the $\sqrt{3}\times\sqrt{3}$-$R30°$ and/or (3×3) and (1×1) domains, respectively [Fig. 3(d)]. Two-third and one-third of all adsorbed OH groups will therefore be in the $\sqrt{3}\times\sqrt{3}$-$R30°$ and/or (3×3) and (1×1) domains, respectively. We can account for such a mixed OH overlayer by combining the results of separate 2/3 ML ($\sqrt{3}\times\sqrt{3}$-$R30°$ domain) and 1 ML $(1\times1$ domain) calculations. With this procedure we find that the OH chemisorption energy is 2.52 eV per OH. Thus it is energetically more favorable to partition 3/4 ML OH into $\sqrt{3}\times\sqrt{3}$-$R30°$ 2/3 ML and (1×1) domains than to have a uniform surface coverage of 3/4 ML.

At 1 ML coverage OH forms a rather interesting overlayer with a chemisorption energy of 2.50 eV per OH. Hydroxyls bind to top sites and point in between two antecedent hydroxyls [Fig. 3(e)]. This is different behavior to that observed at slightly lower coverages where OH groups point directly at O atoms of antecedent hydroxyls. A 1 ML phase of this type is only 0.07 eV less stable than the favored structure. The favored structure can be viewed as a two-dimensional network of hydroxyls rather than the chains which are observed at slightly lower coverages. A structural model for the experimentally observed (1×1) domains was not proposed.[4] Since this [Fig. 3(e)] is the most stable 1 ML OH phase calculated, it is likely that this structure closely models the experimentally observed (1×1) domains.

TABLE III. Chemisorption energies and selected structural parameters for high coverage (1/2 ML→1 ML) OH adsorption on Pt(111). $O_\perp$ and α refer to the O surface distance and the surface O–H angle, respectively. $O–H_{bond}$ values are the closest H bond contacts between neighboring OH groups. At 3/4 ML OH groups are inequivalent. (a) lists average values for the two OH groups in the 2×1 OH chains and (b) refers to the other type of OH group in this phase [Fig. 3(c)].

Coverage (ML)	E_{ads} (eV)	O–H (Å)	O–Pt (Å)	$O–H_{bond}$ (Å)	α (°)
1/2	2.49	0.99	2.00	1.90	108
2/3	2.53	1.00	2.00	1.72	105
3/4 (a)	2.44	0.99	2.00	1.96	109
(b)		1.00	1.98	1.68	103
1	2.50	0.99	1.99	2.03	107

B. The intermediate in the H_2O formation reaction

The hydrogen-oxidation to H_2O reaction on Pt is one of the oldest and most fundamental reactions in catalysis. The nature of the intermediate through which it proceeds has been intensively debated over the years.[12–23] As discussed earlier, the intermediate has been identified as the species that forms through the disproportionation of two H_2O molecules and one adsorbed O [reaction (1)] and assigned as OH.[3,4] It has been shown that this species with a surface coverage of 3/4 ML arranges upon the surface in majority $\sqrt{3}\times\sqrt{3}$-$R30°$ and/or (3×3) domains and minority (1×1) domains. From reaction (1), H atoms, which have never been observed, should also be present on the surface. Having discussed the structure and energetics of pure OH overlayers we now consider the adsorption of H within such overlayers.

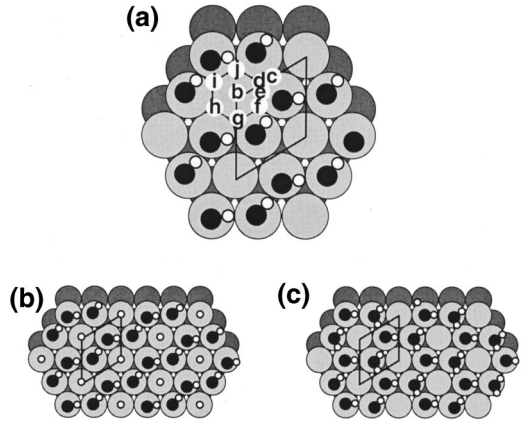

FIG. 4. (a) OH+H coadsorption systems with *b-j* being the possible H positions considered. (b) and (c) are the two types of optimized structure obtained from the nine initial coadsorption systems. (b) is an OH+H coadsorbed phase. (c) is a mixed OH+H_2O phase.

Experimentally H_2O and O react on Pt(111) with a 2:1 stoichiometry to produce a surface overlayer consisting of majority $\sqrt{3}\times\sqrt{3}$-$R30°$ and/or (3×3) domains and minority (1×1) domains.[4] H atoms must be adsorbed within these domains. Since the (1×1) OH phases have a coverage of 1 ML the surface is very crowded in these regions. Every surface Pt atom is directly bonded to an OH and based on a bonding competition argument H atoms will not bond strongly to the surface in these regions.[39,40] H atoms will, therefore, be adsorbed within the majority $\sqrt{3}\times\sqrt{3}$-$R30°$ and/or (3×3)-OH domains. As with the adsorption of pure OH overlayers, we have considered OH+H coadsorption within $\sqrt{3}\times\sqrt{3}$-$R30°$ domains and not the (3×3) domains. The 2:1 stoichiometry of reaction (1) dictates that there should be one adsorbed H for every 3 OH groups. Since, as mentioned earlier, two-third of all adsorbed hydroxyls are located within the $\sqrt{3}\times\sqrt{3}$-$R30°$ and/or (3×3) domains the addition of a single H to the $\sqrt{3}\times\sqrt{3}$-$R30°$ unit cell is equivalent to the addition of one H for every three hydroxyls.

Nine different locations for a single H atom within the 2/3 ML$\sqrt{3}\times\sqrt{3}$-$R30°$ OH phase were calculated separately. The nine initial H locations are labeled ''b'' to ''f'' in Fig. 4(a). After structure optimization of all nine systems, only two types of minima were identified. Examples of which, labeled (b) and (c), are shown in Figs. 4(b) and 4(c). Optimized structural parameters for systems (b) and (c) of Fig. 4 are listed in Table IV. In structure (b) of Fig. 4, H is chemisorbed on the top site of the only Pt atom which is not directly bonded to an OH group. The structure of the $\sqrt{3}\times\sqrt{3}$-$R30°$OH phase in this system is similar to that in the absence of coadsorbed H [Fig. 3(b)]. The H–Pt bond length of 1.55 Å and the H chemisorption energy of 2.8 eV are typical for H chemisorption on clean Pt.[24] This indicates that in coadsorption system (b) of Fig. 4 there is little interaction between chemisorbed H and the OH phase. Figure 4(b) shows a possible structure for the experimentally observed $\sqrt{3}\times\sqrt{3}$-$R30°$ domains but structure (c) of Fig. 4 is more likely, not least because structure (c) of Fig. 4 is 1.18 eV more stable that structure (b). In structure (c) the H atoms are incorporated into the $\sqrt{3}\times\sqrt{3}$-$R30°$OH phase with the effect that every second OH is converted into H_2O. Thus it is OH+H_2O which is chemically different from 2OH+H coadsorbed. This $\sqrt{3}\times\sqrt{3}$-$R30°$OH+H_2O phase with a 1:1 ratio of H_2O and OH is a two-dimensional network with every OH fragment being both a H bond acceptor and donor. The conversion of every second OH into H_2O transforms the OH ''chains'' into OH+H_2O ''rings'' with every O atom coordinated to three H atoms [Fig. 4(c)].

TABLE IV. Selected structural parameters for the two optimized $\sqrt{3}\times\sqrt{3}$-$R30°$ phases, (b) and (c) of Fig. 4, which are possibly the true nature of the experimentally observed $\sqrt{3}\times\sqrt{3}$-$R30°$ domains. $O_\perp$ and α refer to the O surface distance and the surface O–H angle, respectively. $O–H_{bond}$ values are the closest H bond contacts between neighboring OH groups. In structure (c) Ha of H_2O is the H atom of the original OH in this phase and Hb of H_2O is the additional H which was initially chemisorbed.

Structure	H–Pt (Å)	O–H (Å)	O–Pt (Å)	$O–H_{bond}$ (Å)	α (degrees)
(b)	1.55	1.00	2.00	1.69	103
(c) OH		0.98	2.11	2.11	105
H_2O:Ha	2.57	0.99	2.17	1.94	103
:Hb	2.59	1.07		1.48	96

There are several pieces of evidence which point to structure (c) of Fig. 4, i.e., the mixed OH+H_2O phase, as the intermediate in the H_2O formation reaction:

(i) The location of the O atoms of the hydroxyls matches the STM images and also matches the LEED patterns of Ref. 4. (In both STM and LEED the hydrogen atoms of the adsorbed hydroxyls are not observed.) The only other phases which match these images are structure (b) of Fig. 4 (coadsorbed OH and H) or a pure 2/3 ML$\sqrt{3}\times\sqrt{3}$-$R30°$OH phase [Fig. 3(b)]. Both are unlikely since structure (b) of Fig. 4 is 1.18 eV less stable than structure (c) of Fig. 4 and the pure 2/3 ML OH overlayer does not have the correct number of H atoms.

(ii) As discussed above, this phase is formed through the disproportionation of $2H_2O$ molecules and one chemisorbed O which is part of a $p(2\times2)$O overlayer. To form structure (b) of Fig. 4 or *any* other coadsorption of OH and H at some stage, a H_2O molecule must dissociate over a clean Pt site. There is no evidence either from experiment or theory for the dissociation of H_2O on clean Pt. In fact, DFT computed barriers for the dissociation of isolated H_2O molecules and H_2O molecules in mixed OH+H_2O overlayers are ~0.7 and ~1.7 eV, respectively.[41,42] Such high barriers will be insurmountable at the low temperatures (110 K) at which the H_2O formation reaction can proceed.

(iii) We have performed a vibrational analysis on structures (b) and (c) of Fig. 4 and also the pure 2/3 ML$\sqrt{3}\times\sqrt{3}$-$R30°$OH phase [Fig. 3(b)]. Table V lists observed experimental modes from the HREELS spectra of Ref. 4 and their corresponding calculated modes in systems (b) and (c) and also the pure 2/3 ML$\sqrt{3}\times\sqrt{3}$-$R30°$OH phase. From Table V it is clear that the best agreement between experimental modes and calculated modes is obtained with the

TABLE V. Experimental and calculated vibrational modes and their assignments for the observed intermediate in the H_2O formation reaction and three possible structures of this intermediate. $\sqrt{3}\times\sqrt{3}$-$R30°$-$(OH+H_2O)$ corresponds to the phase shown in Fig. 4(c); $\sqrt{3}\times\sqrt{3}$-$R30°$-(2OH) to that shown in Fig. 3(c) and $\sqrt{3}\times\sqrt{3}$-$R30°$-(2OH+H) to that shown in Fig. 4(b). All values are in wave numbers. ν, δ, and T refer to stretching, bending, and translational modes, respectively. $\perp$ and $\parallel$ modes are relative to the OH surface plane or the H_2O surface plane.

Experiment[a]	$\sqrt{3}\times\sqrt{3}$-$R30°$-$(OH+H_2O)$ (c)	$\sqrt{3}\times\sqrt{3}$-$R30°$-(2OH+H) (b)	$\sqrt{3}\times\sqrt{3}$-$R30°$-(2OH)
3476 ν(OH)	3329 ν(OH)	2867,2792 ν(OH)	2856,2782 ν(OH)
1024 $\delta_{\parallel 1}$(OH)	1036 $\delta_{\parallel}$(OH)+$\delta_{\perp}$(H_2O)	1399,1123 $\delta_{\parallel}$(OH)	1160,1139 $\delta_{\parallel}$(OH)
911 $\delta_{\parallel 2}$(OH)	986 $\delta_{\perp}$(H_2O)	⋯	⋯
823 $\delta_{\parallel 3}$(OH)	831 $\delta_{\parallel}$(OH)+$\delta_{\parallel}$(H_2O)	⋯	⋯
436 ν(Pt–OH)	436 ν(Pt–OH)	433 ν(Pt–OH)	530,488 ν(Pt–OH)
347 $T_{\parallel}$(Pt–OH)	244 $T_{\parallel}$(Pt–OH)	271 $T_{\perp}$(Pt–OH)	241 $T_{\perp}$(Pt–OH)
234 $T_{\perp}$(Pt–OH)	154 $T_{\perp}$(Pt–OH)	236 $T_{\parallel}$(Pt–OH)	201 $T_{\parallel}$(Pt–OH)

[a]Reference 4.

mixed OH+H_2O phase [Fig. 4(c)]. Let us in brief consider each mode: In the OH stretching region an experimental mode is observed at 3476 cm^{-1}. In our calculated systems neither the OH+H phase (c) nor the pure OH phase exhibit OH stretching modes above 2900 cm^{-1}. The mixed OH+H_2O phase (c), however, exhibits an OH stretching mode at 3329 cm^{-1} which is within 4% of the experimental value. In the OH bending region three experimental modes are observed (1024 cm^{-1}, 911 cm^{-1}, and 823 cm^{-1}). A single OH configuration could not have three dipole active bending modes. (Chemisorbed hydroxyls which are inclined to the surface normal should exhibit only one dipole active bending mode.) Hence, this observation lead to the suggestion that structurally modified OH groups which experienced different degrees of H bonding accounted for the two additional bending modes (911 cm^{-1} and 823 cm^{-1}).[4] We cannot rule out this possibility. However, if the observed experimental phase was the mixed OH+H_2O phase [Fig. 4(c)] and not a pure OH phase or OH+H [Fig. 4(b)], then it would be possible to have three dipole active bending modes and there would be no need to consider structurally modified hydroxyls. In addition, there is quite good agreement between all three calculated bending modes of the mixed OH+H_2O phase and the three experimentally observed bending modes. The value of the O–Pt stretch in the mixed OH+H_2O phase [Fig. 4(c)] agrees exactly with experiment. For completeness, calculated values of adsorbate translational modes are also included in Table V. For these modes agreement between the calculated values and the experimental values is poor. This is because, in order to calculate accurate values for these modes, surface relaxation should be taken into account. Finally, considering one additional aspect of the HREEL data. If the experimentally observed phase was indeed mixed OH+H_2O, one may expect to observe an HOH scissors mode at $\sim$ 1600 cm^{-1}. Such a mode has not been observed experimentally. This seems to be inconsistent with the mixed OH+H_2O phase. However, in this phase which contains only 1/3 ML H_2O, each H_2O molecule lies quite flat upon the surface (H_2O is inclined by 80° to the surface normal; Table IV). The scissors mode of H_2O molecules in such an orientation will not exhibit a significant dipole moment change in the surface normal and will consequently be difficult to observe.

White and co-workers previously speculated that a mixed OH+H_2O overlayer may be the nature of the intermediate[17] although they later opted for OH.[18] They cited as evidence the fact that H_2O dissociation on clean Pt has not been observed. Further, they argued that the spectroscopic data used in the assignment of pure OH were not inconsistent with a mixed OH+H_2O overlayer.

Considering the above points, we believe that the much debated intermediate in the H_2O formation reaction on Pt(111) is a mixed OH+H_2O phase. In the majority $\sqrt{3}\times\sqrt{3}$-$R30°$ domains there is a local 1:1 ratio of OH and H_2O [Fig. 4(c)]. Taking into account the minority (1×1) pure OH domains then at a macroscopic level the overlayer has a 2:1 ratio of OH and H_2O. Since this is the overlayer produced by the coadsorption of H_2O and O at 100 K followed by annealing to 150 K, this method should be reconsidered as a method to produce chemisorbed OH on Pt(111). It is possible that the minority (1×1) domains are the only *pure* OH phases observed Pt(111).

IV. SUMMARY

(1) At low coverages (1/9 to 1/3 ML) OH binds preferentially at bridge and top sites with a chemisorption energy of approximately 2.25 eV.
(2) At high coverages (1/2 ML to 1 ML) the formation of OH networks causes: (i) a 15% enhancement in OH chemisorption energy; and (ii) a strong preference for OH adsorption at top sites.
(3) Isolated OH groups can diffuse very easily across the Pt(111) surface. This coupled with H bonding between neighboring OH groups indicates that hydroxyls are susceptible to island formation at low coverages.
(4) The species formed using a standard method to produce

adsorbed OH on Pt(111), which is also the intermediate in the water formation reaction, may not be pure OH. We believe it is a mixed $OH+H_2O$ overlayer with an overall surface coverage of 3/4 ML in a 2:1 ratio of OH and H_2O. The $\sqrt{3}\times\sqrt{3}$-$R30°$ domains of this overlayer are $OH+H_2O$ phases in a 1:1 ratio of OH and H_2O with a local coverage of 2/3 ML of O containing species. The (1×1) domains are pure OH regions.

ACKNOWLEDGMENTS

Sincere thanks to The Supercomputing Center for Ireland for computer time. A.M. wishes to thank EPSRC for a studentship. Dr. Joost Wintterlin and Professor Gerhard Ertl are thanked for helpful discussions and communications.

[1] G. B. Fisher and B. A. Sexton, Phys. Rev. Lett. **44**, 683 (1980).
[2] J. R. Creighton and J. M. White, Surf. Sci. **122**, L648 (1982).
[3] S. Völkening, K. Bedurftig, K. Jacobi, J. Wintterlin, and G. Ertl, Phys. Rev. Lett. **83**, 2672 (1999).
[4] K. Bedurftig, S. Völkening, Y. Wang, J. Wintterlin, K. Jacobi, and G. Ertl, J. Phys. Chem. B **103**, 1084 (1999).
[5] J. R. Creighton and J. M. White, Surf. Sci. **136**, 449 (1984).
[6] F. T. Wagner and T. E. Moylan, Surf. Sci. **191**, 121 (1987).
[7] G. Gilarowski, W. Erley, and H. Ibach, Surf. Sci. **351**, 156 (1996).
[8] A. V. Melo, W. E. O'Grady, G. S. Chottiner, and R. W. Hoffman, Appl. Surf. Sci. **21**, 160 (1985).
[9] P. A. Thiel and T. E. Madey, Surf. Sci. Rep. **7**, 211 (1987).
[10] M. Faraday, *Experimental Researches in Electricity, 1844*; or in *Great Books of the Western World*, Vol. 145 (Encyclopaedia Britannica, Chicago, IL, 1952).
[11] J. J. Berzelius, *Jahres-Bericht über die Fortschritte der Physichen Wissenschafter der Physichen Wissenschaften* (H. Laupp, Tübinger, 1836), Vol. 15.
[12] P. R. Norton, in *The Chemical Physics of Solid Surfaces and Heterogeneous Catalysis*, Vol. 4, edited by D. A. King and D. P. Woodruff (Elsevier, Amsterdam, 1982).
[13] G. B. Fisher, J. L. Gland, and S. J. Schmieg, J. Vac. Sci. Technol. **20**, 518 (1982).
[14] J. L. Gland, G. B. Fisher, and E. B. Kollin, J. Catal. **77**, 263 (1982).
[15] A. B. Anton and D. C. Cadogan, Surf. Sci. **239**, L548 (1990).
[16] K. M. Ogle and J. M. White, Surf. Sci. **139**, 43 (1984).
[17] G. E. Mitchell, S. Akhter, and J. M. White, Surf. Sci. **166**, 283 (1986).
[18] G. E. Mitchell and J. M. White, Chem. Phys. Lett. **135**, 84 (1987).
[19] T. A. Germer and W. Ho, Chem. Phys. Lett. **163**, 449 (1989).
[20] B. Hellsing, B. Kasemo, and V. P. Zhdanov, J. Catal. **132**, 210 (1991).
[21] L. K. Verheij, M. Freitag, M. B. Hugenschmidt, I. Kempf, B. Poelsema, and G. Comsa, Surf. Sci. **272**, 276 (1992).
[22] L. K. Verheij, Surf. Sci. **371**, 100 (1997).
[23] L. K. Verheij and M. B. Hugenschmidt, Surf. Sci. **416**, 37 (1998).
[24] G. Papoian, J. K. Nørskov, and R. Hoffmann, J. Am. Chem. Soc. **17**, 4129 (2000).
[25] A. Michaelides and P. Hu, Surf. Sci. **437**, 362 (1999).
[26] A. Michaelides and P. Hu, J. Chem. Phys. **112**, 6006 (2000).
[27] A. Michaelides, P. Hu, and A. Alavi, J. Chem. Phys. **111**, 1343 (1999).
[28] A. Michaelides and P. Hu, J. Chem. Phys. **112**, 8120 (2000).
[29] M. T. M. Koper and R. A. van Santen, J. Electroanal. Chem. **472**, 126 (1999).
[30] K. Hermann, M. Witko, L. G. M. Pettersson, and P. Siegbahn, J. Chem. Phys. **610**, 99 (1993).
[31] H. Yang and J. L. Whitten, J. Phys. Chem. B **101**, 4090 (1997).
[32] H. Yang and J. L. Whitten, Surf. Sci. **370**, 136 (1997).
[33] E. M. Patrito, P. Paredas Olivera, and H. Sellers, Surf. Sci. **306**, 447 (1994).
[34] M. C. Payne, M. P. Teter, D. C. Allan, T. A Arias, and J. D. Joannopoulos, Rev. Mod. Phys. **64**, 1045 (1992).
[35] D. Vanderbilt, Phys. Rev. B **41**, 7892 (1990).
[36] J. P. Perdew, V. A. Chevary, S. H. Vosko, K. A. Jackson, M. R. Pederson, D. J. Singh, and C. Fiolhais, Phys. Rev. B **46**, 6671 (1992).
[37] H. J. Monkhorst and J. D. Pack, Phys. Rev. B **13**, 5188 (1976).
[38] A. Michaelides and P. Hu (unpublished).
[39] K. Bleakley and P. Hu, J. Am. Chem. Soc. **121**, 7644 (1999).
[40] C. J. Zhang, P. Hu, and M.-H. Lee, Surf. Sci. **432**, 305 (1999).
[41] A. Michaelides and P. Hu, J. Am. Chem. Soc. **40**, 9866 (2000).
[42] A. Michaelides and P. Hu (unpublished).